AIP Applied Physics Letters

Nanometer-scale conversion of Si 3 N 4 to SiO x

F. S.-S. Chien, J.-W. Chang, S.-W. Lin, Y.-C. Chou, T. T. Chen, S. Gwo, T.-S. Chao, and W.-F. Hsieh

Citation: Applied Physics Letters **76**, 360 (2000); doi: 10.1063/1.125754
View online: http://dx.doi.org/10.1063/1.125754
View Table of Contents: http://scitation.aip.org/content/aip/journal/apl/76/3?ver=pdfcov
Published by the AIP Publishing

Articles you may be interested in
Reaction pathways in remote plasma nitridation of ultrathin SiO 2 films
J. Appl. Phys. **91**, 48 (2002); 10.1063/1.1419208

Improved Auger electron spectroscopy sputter depth profiling of W/WN x and WSi x layers on Si substrates
J. Vac. Sci. Technol. A **19**, 2174 (2001); 10.1116/1.1378073

Nitridation of thermal SiO 2 films by radio-frequency plasma assisted electron cyclotron resonance: Layer structure and composition
J. Vac. Sci. Technol. A **19**, 17 (2001); 10.1116/1.1333084

Nitridation of thermal SiO 2 films by radio-frequency plasma assisted electron cyclotron resonance: Effect of plasma modes and process parameters
J. Vac. Sci. Technol. A **19**, 9 (2001); 10.1116/1.1331295

SiO 2 thickness determination by x-ray photoelectron spectroscopy, Auger electron spectroscopy, secondary ion mass spectrometry, Rutherford backscattering, transmission electron microscopy, and ellipsometry
J. Vac. Sci. Technol. B **18**, 440 (2000); 10.1116/1.591208

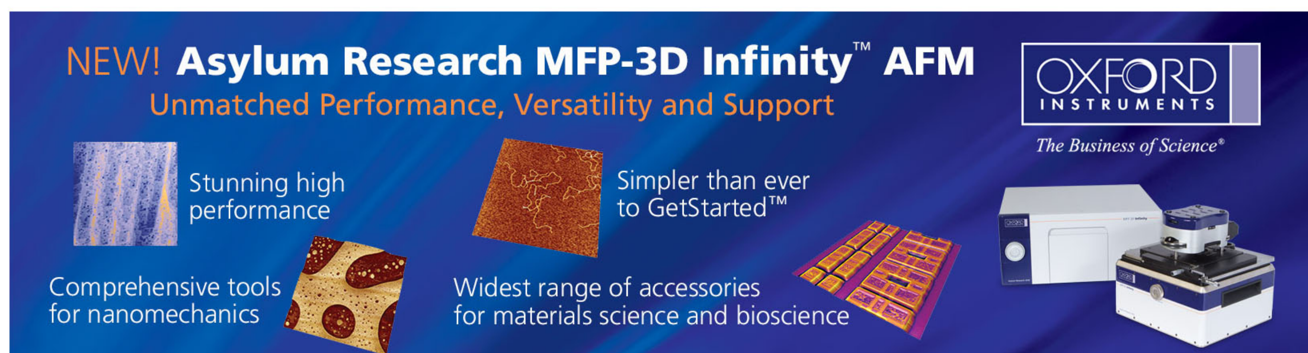

This article is copyrighted as indicated in the article. Reuse of AIP content is subject to the terms at: http://scitation.aip.org/termsconditions. Downloaded to IP: 140.113.38.11 On: Thu, 01 May 2014 08:00:35

Nanometer-scale conversion of Si_3N_4 to SiO_x

F. S.-S. Chien,[a] J.-W. Chang, S.-W. Lin, Y.-C. Chou, T. T. Chen, and S. Gwo[b]
Department of Physics, National Tsing-Hua University, Hsinchu 300, Taiwan, Republic of China

T.-S. Chao
National Nano Device Laboratory, 1001-1 Ta Hsueh Road, Hsinchu 300, Taiwan, Republic of China

W.-F. Hsieh
Institute of Electro-Optical Engineering, National Chiao-Tung University, Hsinchu 300, Taiwan, Republic of China

(Received 18 October 1999; accepted for publication 16 November 1999)

It has been found that atomic force microscope (AFM) induced local oxidation is an effective way for converting thin (<5 nm) Si_3N_4 films to SiO_x. The threshold voltage for the 4.2 nm film is as low as 5 V and the initial growth rate is on the order of 10^3 nm/s at 10 V. Micro-Auger analysis of the selectively oxidized region revealed the formation of SiO_x. Due to the large chemical selectivity in various etchants and great thermal oxidation rate difference between Si_3N_4, SiO_2, and Si, AFM patterning of Si_3N_4 films can be a promising method for fabricating nanoscale structures. © *2000 American Institute of Physics.* [S0003-6951(00)03003-5]

Silicon dioxide (SiO_2) and silicon nitride (Si_3N_4) are the two most important dielectric materials for the microelectronic processing. In contrast to SiO_2, Si_3N_4 has many unique electrical, optical, mechanical, and chemical properties. For example, it has a larger dielectric constant (7.5 vs 3.9), a larger refractive index (2.05 vs 1.46), and a larger density (3.1 vs 2.2 g/cm^3).[1] On the other hand, SiO_2 films are preferably used in the circumstances where a large band gap (9 vs $\sim$5 eV) is necessary for electrical insulation. And, Si–SiO_2 interfaces display better device properties than that of Si–Si_3N_4 interfaces. As the scaling of ultralarge-scale integrated circuits continues into the nanometer regime (<100 nm) to achieve high levels of integration and speed, ultrathin SiO_2 gate dielectrics of $\sim$2–3 nm thick become necessary.[2] To reduce the problem of direct tunneling in the case of ultrathin SiO_2, physically thicker insulators with higher dielectric constants are more favorable as the gate dielectrics. Therefore, silicon nitride and silicon oxynitride (SiO_xN_y) thin films are particularly interesting for the ultrathin dielectric applications. In this letter, we present an approach of locally converting ultrathin (<5 nm) Si_3N_4 to SiO_x or SiO_xN_y with an atomic force microscope (AFM).

The chemical selectivity between these two materials is also very important for the mask applications. For example, Si_3N_4 oxidizes slowly, about 50 times less than Si when using wet oxidation at 1100 °C.[3] Therefore, it is often used as a mask against O_2 diffusion during the local oxidation of silicon (LOCOS) process. Moreover, Si_3N_4 has highly selective etch rates over SiO_2 and Si in many etchants. Etch rate selectivity of Si_3N_4:SiO_2:Si in diluted HF (40%) at room temperature is about 1:>100:0.1 and selectivity of Si_3N_4:SiO_2:Si in 94.5% H_3PO_4 at 180 °C is about 10:<1:0.3.[4,5] Using an anisotropic aqueous KOH (30 wt %) etchant, typically used for wet bulk micromachining, selectivity of Si_3N_4:SiO_2:Si(100) at 60 °C is about 1:>14:>2600.[4] As a result, AFM selective-oxidized Si_3N_4 films can be excellent nanoscale etch masks both for positive- and negative-type pattern transfers depending on the etchant combination.

Previous reported results of AFM-induced oxidation have been limited to semiconductors and metals.[6–13] However, it is not necessary that the modified surface is conductive. Even if there is a thin insulating film grown on the conductive substrate, the intense electrical field between the probe and the substrate still can drive the oxidant anions (most likely OH^-) to diffuse into the thin dielectric film (Si_3N_4 in this work). The reaction of oxidants and silicon nitride results in the replacement of nitrogen by oxygen. Hence, the local intensive field induced by an AFM probe can turn silicon nitride into silicon oxides or silicon oxynitrides.

The silicon nitride films were grown on *p*-type, 10 Ω cm, (001)-oriented Si wafers in a low-pressure chemical vapor deposition (LPCVD) reactor at 780 °C using a mixture of $SiCl_2H_2$ and NH_3. Two as-grown film thicknesses of 5 (sample A) and 2.5 nm (sample B) measured by ellipsometry were used for this study. Sample A was further densified by a rapid thermal anneal of 10 s at 1000 °C in a nitrogen gas. The film thickness was reduced to 4.2 nm after annealing. Local electric-field-induced oxidation was performed in ambient using highly doped (0.01–0.025 Ω cm) n^+-Si AFM probes (contact-type Pointprobe®, Nanosensors) and a commercial AFM (*CP* type, Park Scientific Insturments) operating in the contact mode. Both uncoated and PtIr-coated tips have been used. The typical force constant and the resonance frequency of the cantilevers used are 0.2 N/m and 13 kHz, respectively.

Figure 1(a) shows oxidized lines written on the densified sample A with 0.4 nN contact force and 0.1 μm/s scan speed at various sample biases ranging from +4 to +10 V with

[a]Also with: Institute of Electro-Optical Engineering, National Chiao-Tung University, and Center for Measurement Standards, Hsinchu 300, Taiwan, Republic of China.
[b]Author to whom correspondence should be addressed; electronic mail: gwo@phys.nthu.edu.tw

This article is copyrighted as indicated in the article. Reuse of AIP content is subject to the terms at: http://scitation.aip.org/termsconditions. Downloaded to IP: 140.113.38.11 On: Thu, 01 May 2014 08:00:35

 © 2000 American Institute of Physics

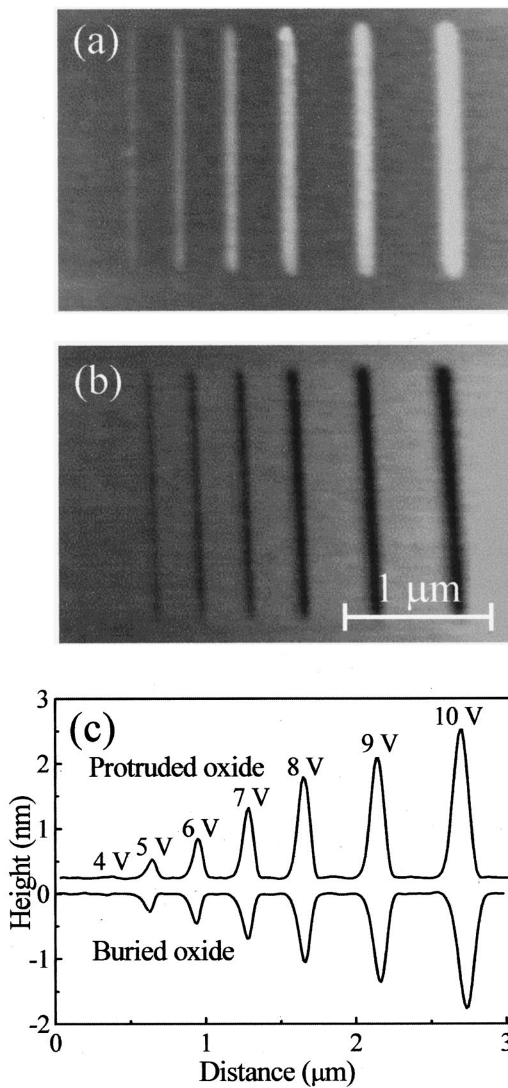

FIG. 1. (a) AFM image of silicon nitride film which shows oxidized lines written on the densified sample A (4.2 nm thickness) with 0.4 nN contact force and 0.1 μm/s scan speed at various sample biases ranging from +4 to +10 V. (b) AFM image of the same area after HF dipping. (c) Cross-sectional profiles of images (a) and (b) showing the heights and depths of the protruded and buried oxides.

respect to the tip. The written lines are topographically protruded since the molar volume of oxide is larger than that of silicon nitride. To verify that the silicon nitride had been converted to silicon oxide, the written sample was dipped into a 1% HF solution for 20 s. In our experiments, the etching rates in 1% HF solution determined by ellipsometry and AFM are ~0.01 nm/s for the densified nitride sample and 0.27 nm/s for the AFM-induced oxide, corresponding to an etch selectivity of 27. Therefore, the protruded appearance of oxidized lines can be converted to trenches after HF dip as shown in Fig. 1(b). Figure 1(c) displays the cross sectional profiles of the protruded and buried parts of oxidized lines at sample biases varying from +4 to +10 V, respectively. No oxidized line was observed as the bias under +5 V. The heights (h), depths (d), and full widths at half maximum (FWHM) of the protruded and buried parts of oxide lines are in proportion to sample biases (see Table I). The volume of buried oxide can be considered as the volume of consumed nitride which was converted into oxide while the sum of the

TABLE I. Protruded height (h), buried depth (d), FWHM, aspect ratio (h/FWHM), and conversion ratio $[(h+d)/d]$ of the AFM-induced oxide on the Si_3N_4 thin film at various biases.

Bias (V)	5	6	7	8	9	10
h (nm)	0.29	0.60	1.09	1.57	1.90	2.33
d (nm)	0.45	0.62	0.86	1.23	1.59	1.98
FWHM (nm)	65	73	80	81	102	118
h/FWHM	0.0045	0.0082	0.0136	0.0194	0.0186	0.0197
$(h+d)/d$	1.64	1.97	2.27	2.28	2.19	2.18

protruded and buried parts as the volume of oxide after conversion. The conversion ratios of oxide volumes to consumed nitride volumes $[(h+d)/d]$ at higher sample biases (>7 V) are around a constant value of 2.23, indicating a nearly complete conversion of nitride film. However, this ratio is much higher than the reported conversion ratio of thermal oxidation of silicon nitride that is around 1.64.[3] This is probably because the AFM-induced oxide is less dense than the thermal oxide.

To investigate the oxide growth rate, voltage pulses of varied height and duration (1–500 ms) were applied to the densified film A and the produced oxide dot arrays were analyzed. We have found that the initial growth rate of AFM-induced oxide depends on the tip characteristics, but typically with a magnitude ranging from 500 to 1500 nm/s.[14] An exponential decay relation of the growth rate with the grown oxide thickness $[dh/dt \propto \exp(-h/L_c)]$ can be found from the kinetic data.[8,9,14] In our experiments, the characteristic decay length L_c (bias and tip dependent) is typically within the range of 0.3–0.6 nm.[14] Compared with the rate coefficient $A \cong 1$ nm/min$^{2/3}$ $(h = A t^{2/3})$ for the wet thermal oxidation at 1100 °C and under 0.95 atm of water vapor,[3] AFM-induced oxidation of Si_3N_4 is much faster than other methods and even faster than the AFM-induced oxidation rate of Si(001) (initial rate of 10 nm/s and $L_c = 0.9$ nm at 10 V).[8] The observed low critical field strengths and high oxidation rates of AFM-induced oxidation on Si_3N_4 imply that the AFM oxidation of Si_3N_4 has an significantly different kinetics from that of common thermal oxidation mechanisms.

Auger electron spectroscopy was also utilized to investigate the chemical composition of the AFM-induced oxide. The Auger spectra taken from the as-grown and AFM-

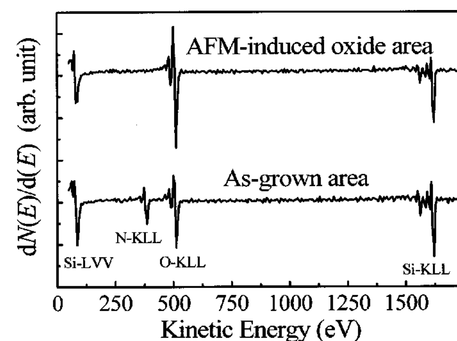

FIG. 2. Micro-Auger spectra of sample B (2.5 nm thickness) silicon nitride film at the as-grown area and the AFM-oxidized area. The peak of N-KLL at ~385 eV on the as-grown area completely disappears on the AFM-oxidized area. And, the magnitude of O-KLL at ~512 eV is much enhanced on the oxidized area as compared to that of the as-grown area.

This article is copyrighted as indicated in the article. Reuse of AIP content is subject to the terms at: http://scitation.aip.org/termsconditions. Downloaded to IP: 140.113.38.11 On: Thu, 01 May 2014 08:00:35

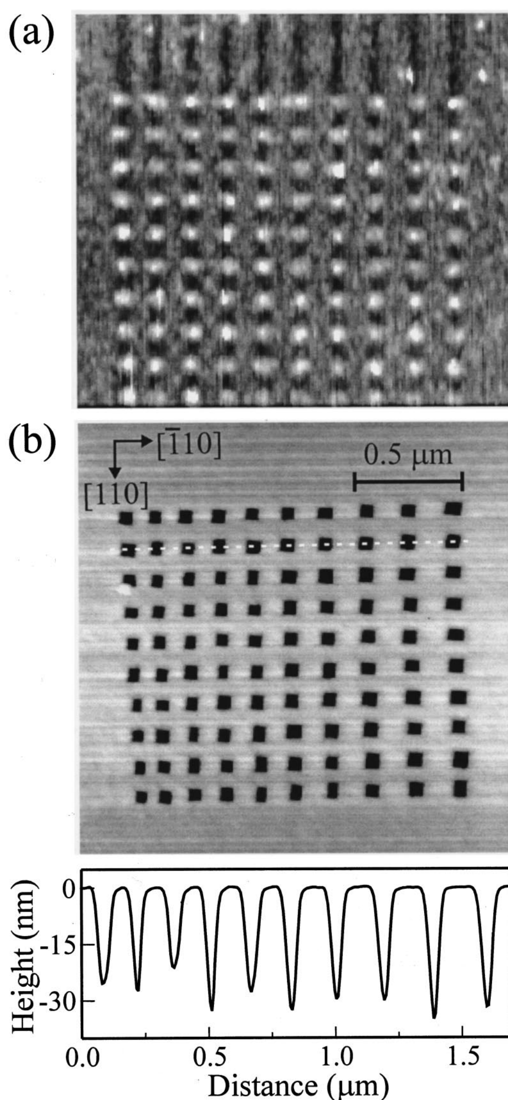

FIG. 3. (a) AFM image of an array of 10×10 silicon oxide dots obtained by applying voltage pulses of +9 V and 5 ms to the 4.2 nm-Si_3N_4/Si(001) film. The average dot diameter and height are 70 and 2 nm. (b) AFM image of the same area after HF dipping (both for oxide stripping and nitride thinning) and KOH anisotropic etching of underlying Si(001). Every oxide dot is converted to a square pit (~50×50–70×70 nm^2) with an inverted pyramidal geometry. (c) Cross-sectional profile of the dashed line shown in (b). The etch depth determined by AFM is ~20–35 nm.

induced oxidized area of sample B are shown in Fig. 2. Both spectra have emission peaks of Si-LVV at ~86 eV, Si-KLL at ~1620 eV, and O-KLL at ~512 eV. However, the peak of N-KLL at ~385 eV on the as-grown area completely disappears on the AFM-oxidized area. Meanwhile, the magnitude of O-KLL is much enhanced on the oxidized area as compared to that of the as-grown area. It is evident that the nitrogen content was thoroughly replaced by the oxygen atoms in the ultrathin film case. The results of Auger electron spectroscopy support the previous suggestion that the nitride films can be turned into oxides by AFM-induced oxidation.[11]

The high growth rate of AFM-induced oxide on Si_3N_4 is very useful for the mask applications. Figure 3(a) shows a 10× 10 oxide dot array on the densified sample A, which was made by applying voltage pulses of +9 V and 5 ms duration to the sample with respect to the tip. The oxide dot formation is very reproducible and is uniform with an average diameter of ~70 nm and a height of ~2 nm. Subsequently, the sample was etched with a HF solution at room temperature and with a 20 wt % KOH solution at ~50 °C for 15 s [Fig. 3(b)]. After pattern transfer, each oxide dot converts to a square pit (~50×50–70×70 nm^2). For the anisotropic etching of (001)-oriented silicon using KOH solution, inverted pyramidal pit (independent of the dot mask shape) is formed with four intersecting {111} crystal planes. The AFM-measured etch depth as shown in Fig. 3(c) is around 20–35 nm. This value is in good agreement with the ideal value determined by the terminal etch geometry (35–50 nm), considering a finite probe size. At present, we have also succeeded in fabricating structures with depths on the order of a few hundred nm using AFM-modified nitride masks of 2–3 nm thick.[14]

In summary, we have demonstrated that AFM-induced local oxidation is a very effective way for converting Si_3N_4 to SiO_x with low threshold voltages and extremely fast oxidation rates. Pattern transfer using AFM-induced Si_3N_4/SiO_x etch mask is now feasible. This is a potentially useful nanolithographic approach because the part of mask functions as etch stop is well structured Si_3N_4 instead of AFM-induced SiO_x.[12,13] Also, it is compatible with the conventional microelectronic processing. The etched structures can be useful for fabricating microstructures, as templates for selective growth of nanostructures, or as high-density read-only memory.

This work was supported by the National Science Council (Contract Nos. NSC 88-2112-M-007-027 and NSC 88-2112-M-007-022), Taiwan, Republic of China.

[1] S. M. Sze, *Physics of Semiconductor Devices*, 2nd ed. (Wiley, New York, 1981), p. 852.
[2] G. Lucovsky, J. Vac. Sci. Technol. A **17**, 1340 (1999).
[3] T. Enomoto, R. Ando, H. Morita, and H. Nakayama, Jpn. J. Appl. Phys. **17**, 1049 (1978).
[4] S. D. Collin, in *Semiconductor Micromachining*, edited by S. A. Campbell and H. J. Lewerenz (Wiley, Chichester, 1998), Vol. 2, Chap. 2.
[5] W. van Gelder and V. E. Hauser, J. Electrochem. Soc. **114**, 869 (1967).
[6] J. A. Dagata, J. Schneir, H. H. Harary, C. J. Evans, M. T. Postek, and J. Bennet, Appl. Phys. Lett. **56**, 2001 (1990).
[7] J. A. Dagata, T. Inoue, J. Itoh, K. Matsumoto, and H. Yokoyama, J. Appl. Phys. **84**, 6891 (1998).
[8] Ph. Avouris, R. Martel, T. Hertel, and R. Sandstrom, Appl. Phys. A: Mater. Sci. Process. **66**, S659 (1998).
[9] R. García, M. Calleja, and F. Pérez-Murano, Appl. Phys. Lett. **72**, 2295 (1998).
[10] H. Sugimura, T. Uchida, N. Kitamura, and H. Masuhara, J. Phys. Chem. **98**, 4352 (1994).
[11] S. Gwo, C.-L. Yeh, P.-F. Chen, Y.-C. Chou, T. T. Chen, T.-S. Chao, S.-F. Hu, and T.-Y. Huang, Appl. Phys. Lett. **74**, 1090 (1999).
[12] E. S. Snow, P. M. Campbell, and P. J. McMarr, Appl. Phys. Lett. **63**, 749 (1993).
[13] F. S.-S. Chien, C. L. Wu, Y.-C. Chou, T. T. Chen, S. Gwo, and W.-F. Hsieh, Appl. Phys. Lett. **75**, 2429 (1999).
[14] F. S.-S. Chien, J.-W. Chang, S.-W. Lin, and S. Gwo (unpublished results).

This article is copyrighted as indicated in the article. Reuse of AIP content is subject to the terms at: http://scitation.aip.org/termsconditions. Downloaded to IP: 140.113.38.11 On: Thu, 01 May 2014 08:00:35